IV International Conference on Computational Methods for Coupled Problems in Science and Engineering
COUPLED PROBLEMS 2011
M. Papadrakakis, E. Oñate and B. Schrefler (Eds)

MODELLING OF SIMULTANEOUS INDUCTION HARDENING IN MONOLITHIC FORMULATION

PAVEL KARBAN[*], IVO DOLEŽEL[†] AND BOHUŠ ULRYCH[*]

[*] Faculty of Electrical Engineering
University of West Bohemia
Univerzitní 16, 306 14 Plzeň
e-mail: {karban, ulrych}@kte.zcu.cz

[†] Faculty of Electrical Engineering
Czech Technical University
Technická 2, 166 27 Praha 6
email: dolezel@fel.cvut.cz

Key words: Induction Hardening, Nonlinear Coupled Problem, Monolithic Formulation, Numerical Analysis, Electromagnetic Field, Temperature Field.

Abstract. Induction hardening of an axisymmetric steel workpiece is modeled. This evolutionary and highly nonlinear process is solved by a fully adaptive higher-order finite element method. Numerical computations are realized in the monolithic formulation, using own code Hermes. All nonlinear dependencies of material properties on temperature are respected. The methodology is illustrated by a typical example whose results are discussed.

1 INTRODUCTION

Hardening of steel bodies is a widely used metallurgical process whose purpose is to bring about local changes in the crystalline structure of its surface layers resulting in their higher hardness. The part of the body to be hardened is first heated somewhat above temperature Ac_3 when steel forms a uniform austenite structure. Then, after eventual equalization of temperatures, the body must intensively be cooled by a suitable quenchant. The result is harder, but more brittle martensite structure of the hardened part. The structure of steel in internal layers remains unchanged.

From the physical viewpoint, modeling of this process is still represents a challenge because it represents a strongly nonlinear and evolutionary coupled problem. It includes generation of magnetic field, production of the Joule losses in the processed object, its heating and consequent cooling accompanied by metallurgical changes in its surface structure. Papers that are aimed at the relevant simulations are rather rare [1–4], and usually respect only the nonlinearity of the magnetic permeability.

The authors present a numerical solution to the problem that takes into account all material nonlinearities (most of the material properties are considered as nonlinear functions of the temperature). The solution itself is performed by a fully adaptive higher-order finite element method in the monolithic formulation and realized by own code Hermes [5].

2 FORMULATION OF THE PROBLEM

Consider an arbitrary axisymmetric steel body, whose surface is to be locally hardened, see Fig. 1. The hardened part is placed in the inductor connected to a current source providing harmonic current of amplitude I and frequency f. These parameters have to be sufficient enough for heating the surface to the prescribed temperature in a reasonable time.

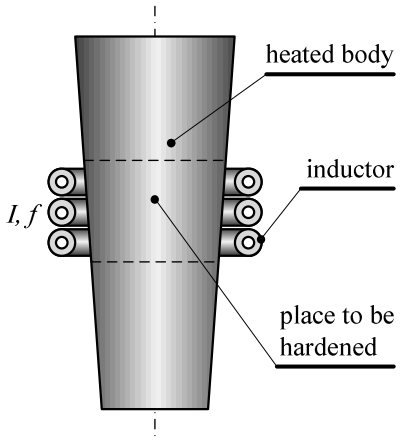

Figure 1: Hardening of axisymmertric bodies

The task is to model the process with the following aims:

- to find the time evolution of the surface temperature in the hardened region,
- to find the time evolution of the cooling process and its velocity, and
- to determine the distribution of the resultant hardness.

3 CONTINUOUS MATHEMATICAL MODEL OF THE PROCESS

The mathematical model of the problem is given by two nonlinear and nonstationary partial differential equations (PDEs) describing distribution of the magnetic and temperature fields. These equations have to be supplemented with correct boundary conditions.

Magnetic field is described by the well-known parabolic equation for magnetic vector potential $\boldsymbol{A}$ in the form

$$\operatorname{curl}\left(\frac{1}{\mu}\operatorname{curl}\boldsymbol{A}\right)+\gamma\frac{\partial\boldsymbol{A}}{\partial t}=\boldsymbol{J}_{\mathrm{ext}}\,, \tag{1}$$

where μ denotes the magnetic permeability, γ the electric conductivity and $\boldsymbol{J}_{\mathrm{ext}}$ the vector of the external harmonic current density in the inductor.

But solution to equation (1) is, in this case, practically unfeasible. The reason consists in the deep disproportion between the frequency f (on the order of kHz) of the field current I and time of heating t_{h} (seconds or tens of seconds). That is why the model was somewhat simplified using the assumption that the magnetic field is harmonic. In such a case it can be described by the Helmholtz equation for the phasor $\underline{\boldsymbol{A}}$ of the magnetic vector potential $\boldsymbol{A}$ [6]

$$\operatorname{curl}\left(\operatorname{curl}\underline{\boldsymbol{A}}\right)+\mathrm{j}\cdot\omega\gamma\mu\underline{\boldsymbol{A}}=\mu\underline{\boldsymbol{J}}_{\mathrm{ext}}\,, \tag{2}$$

where ω is the angular frequency. But the magnetic permeability of ferromagnetic parts is always assigned to the local value of magnetic flux density. It computation is, in such a case, based on an iterative method.

The conditions along the axis of the device and artificial boundary placed at a sufficient distance from the system are of the Dirichlet type ($\underline{\boldsymbol{A}} = \underline{\mathbf{0}}$).

Temperature field is described by the heat transfer equation [7]

$$\operatorname{div}\left(\lambda \cdot \operatorname{grad} T\right) = \rho c_{\mathrm{p}} \cdot \frac{\partial T}{\partial t} - p\,, \tag{3}$$

where λ is the thermal conductivity, ρ the mass density and c the specific heat (all of these parameters are temperature-dependent functions). Finally, symbol p denotes the time average internal volumetric sources of heat that generally consist of the volume Joule losses p_{J} due to eddy currents and magnetization losses p_{m}. Thus, we can put

$$p = p_{\mathrm{J}} + p_{\mathrm{m}}\,, \tag{4}$$

where

$$p_{\mathrm{J}} = \frac{\left|\underline{\boldsymbol{J}}_{\mathrm{eddy}}\right|^2}{\gamma}, \quad \underline{\boldsymbol{J}}_{\mathrm{eddy}} = \mathrm{j} \cdot \omega \gamma \underline{\boldsymbol{A}}\,, \tag{5}$$

while p_{m} (provided that they are considered) are determined from the known measured loss dependence $p_{\mathrm{m}} = p_{\mathrm{m}}\left(\left|\underline{\boldsymbol{B}}\right|\right)$ for the used steel (magnetic flux density $\boldsymbol{B}$ in every element in this model is harmonic).

During the process of cooling the inductor is switched off, so that the term determining the internal volumetric losses p in (2) vanishes.

The boundary conditions take into account convection and radiation, but their particular application depends on the case solved.

All material parameters (μ, γ, λ, ρc_{p}) occurring in (2) and (3) are nonlinear functions of temperature. As the temperature rise of the heated body in the course of the process ranges from 800–1000 °C, these nonlinearities cannot be neglected, because the error of computation could reach an unacceptable value.

4 NUMERICAL SOLUTION

The numerical solution of the problem is performed by a fully adaptive higher-order finite element method (*hp*-FEM. It is a modern version of the finite element method combining finite elements of variable size (*h*) and polynomial degree (*p*) in order to obtain fast exponential convergence [8].

The automatic adaptation of *hp*-meshes significantly differs from the adaptivity in standard methods of this kind. This implies that traditional error estimates (one number per element) do not provide enough information to guide *hp*-adaptivity. One needs a better knowledge of the distribution of the error function derived from the difference between the exact solution u

and approximate solution u'. This error function may be expressed, for example, by the H^1 norm

$$\|e\|_{H^1} = \left| \int_{\Omega} \left(\delta^2 + (\text{grad}\,\delta) \cdot (\text{grad}\,\delta) \right) \text{d}\Omega \right|^{1/2} \tag{6}$$

where $\delta = |u - u'|$ is the local error of solution obtained in a particular step of the *hp*-process and Ω denotes the definition area of the problem. In principle, error δ could be obtained from the estimates of higher derivatives, but this approach is not very practical. Usually it is easier to use a reference solution, i.e., an approximation u_{ref}, which is at least by one order more accurate than u'. The *hp*-adaptivity is then guided by an a posteriori error estimate of the form $\delta = u_{\text{ref}} - u'$. More details on automatic *hp*-adaptivity on meshes with arbitrary level hanging nodes can be found in [9].

At each time level, optimal meshes are obtained automatically by independent adaptive processes. They change in time as the solution changes, respecting different features of particular fields. This is possible as a result of our own multi-mesh technique that allows us solving multiphysics problems monolithically, even though each physical field is discretized on a geometrically different mesh. Thus, our approach leads to a significant reduction of the size of the discrete problem and speeds up the whole computation [10, 11]. In practical computations all physical fields are solved simultaneously, in a monolithic formulation

Our own numerical software Hermes2D [5] was used for the computation. It is capable of all the features mentioned above, such as the higher-order finite element method, automatic adaptivity on *hp*-meshes or assembling the stiffness matrix on geometrically different meshes.

5 ILLUSTRATIVE EXAMPLE

The methodology will be illustrated by an example of induction hardening of the chuck head of a box-column drilling machine. Its arrangement is depicted in Fig. 2. The chuck is made of steel NZ3. The aim of the process is to harden just the low thin part of the body.

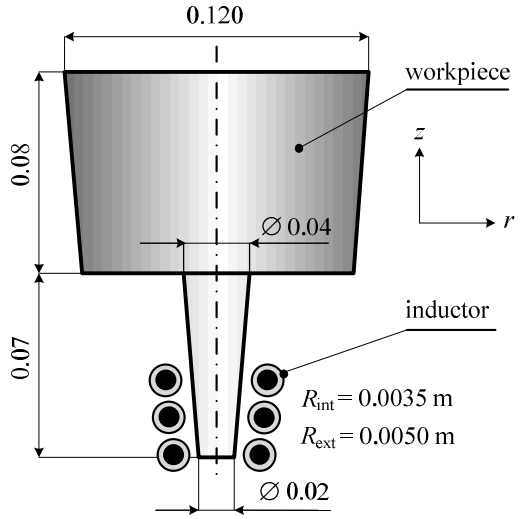

Figure 2: Hardening of axisymmetric bodies (all dimensions in mm)

The inductor (made of a massive hollow copper conductor of circular cross section cooled by water) carries current of density $J_{\text{ext}} = 2\times10^7$ A/m^2 and frequency $f = 10$ kHz. In the course of heating, the process is realized in air of temperature $T_{\text{ext}} = 20\,°\text{C}$ and the generalized coefficient of convective heat transfer (respecting also radiation) $\alpha_{\text{air}} = 20$ W/m^{2}K. In the process of cooling by spraying water of temperature $T_{\text{wat}} = 10\,°\text{C}$, $\alpha_{\text{cool}} = 1200$ W/m^{2}K. The hardening temperature Ac_3 for the considered steel is $873\,°\text{C}$ and the final temperature after cooling characterized by full martensite structure of the hardened layers $T_{\text{M}} = 100\,°\text{C}$. The most important nonlinear characteristics of steel NZ3 are depicted in Figs. 3–7.

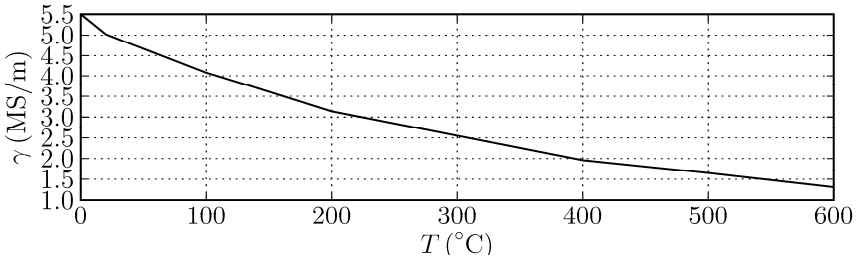

Figure 3: Temperature dependence of electrical conductivity γ (steel NZ3)

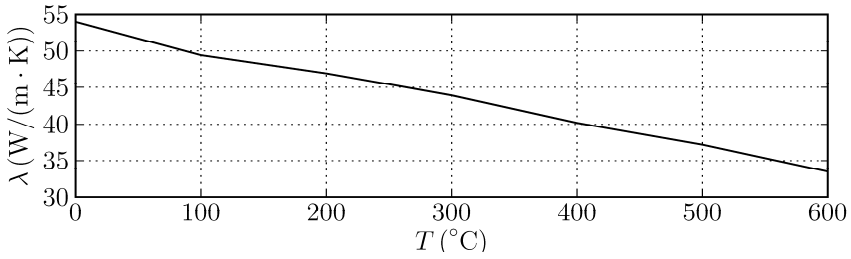

Figure 4: Temperature dependence of thermal conductivity γ (steel NZ3)

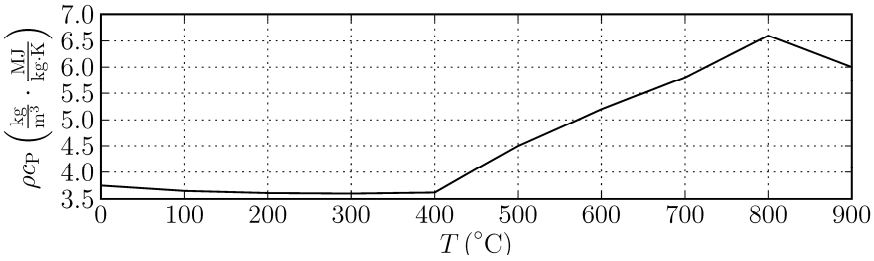

Figure 5: Temperature dependence of heat capacity ρc_{p} (steel NZ3)

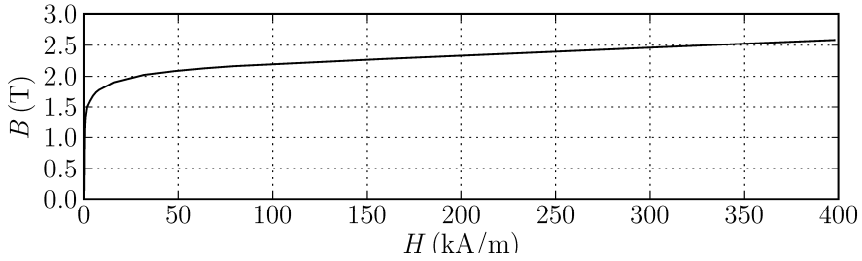

Figure 6: Magnetization characteristic of steel NZ3 (for $T = 20\,°\text{C}$)

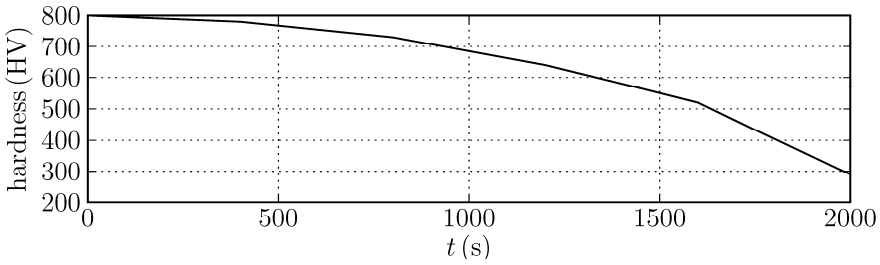

Figure 7: Hardness in HV as a function of the time of cooling

Magnetic permeability μ_r is a function of magnetic flux density and temperature. For every type of steel it must be found experimentally, which usually represents a serious difficulty. We introduce, therefore, an assumption that $\mu_r(B,T) = \mu_r(B,T_0)\cdot\varphi(T)$, where $\mu_r(B,T_0)$ is the dependence of relative permeability on magnetic flux density B at a given temperature T_0 (for example, $T_0 = 20\,°\text{C}$) and function φ is given by the relation

$$\text{for } T_0 \le T \le T_C \quad \varphi(T) = a - bT^2,$$

$$\text{for } T_C \le T \qquad \varphi(T) = \frac{1}{\mu_r(B,T_0)}.$$

Here

$$a = \frac{\mu_r(B,T_0)T_C^2 - T_0^2}{\mu_r(B,T_0)\left(T_C^2 - T_0^2\right)},\quad b = \frac{\mu_r(B,T_0) - 1}{\mu_r(B,T_0)\left(T_C^2 - T_0^2\right)}$$

and T_C is the Curie temperature. For steel NZ3 $T_C = 800\,°\text{C}$ and the function $\varphi(T)$ is depicted in Fig. 8.

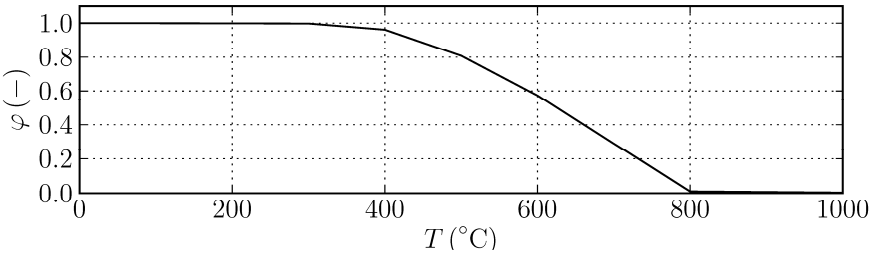

Figure 8: Function $\varphi(T)$ for the temperature correction of magnetic permeability

The discretization mesh for electromagnetic field was composed of about 27000 elements mostly of the second and third orders, while the mesh for temperature field (that was calculated only in the workpiece and turns of the inductor) about 20 000 elements, mostly of the third and fourth orders. After several tests we accepted the time step $\Delta t = 0.25\,\text{s}$. The complete computations of the process ranging to 78 s (when the surface temperature drops to the value of $T_M = 100\,°\text{C}$) took about 3 hours.

Figure 9 shows the discretization mesh in the region of the part to be hardened including the three turns of the inductor.

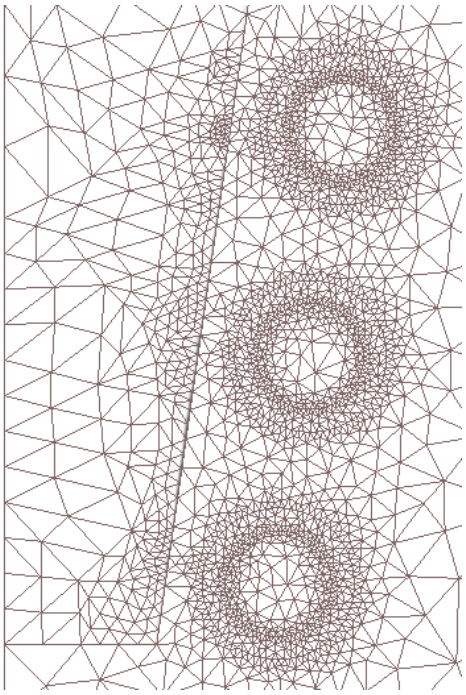

Figure 9: A part of the discretization mesh in the hardened region

Figure 10 shows the surface temperature of the hardened part (measured from the bottom edge of the body in Fig. 2) at several time levels. It is obvious that the austenitization temperature Ac_3 was only exceeded along the first 25 mm of the body.

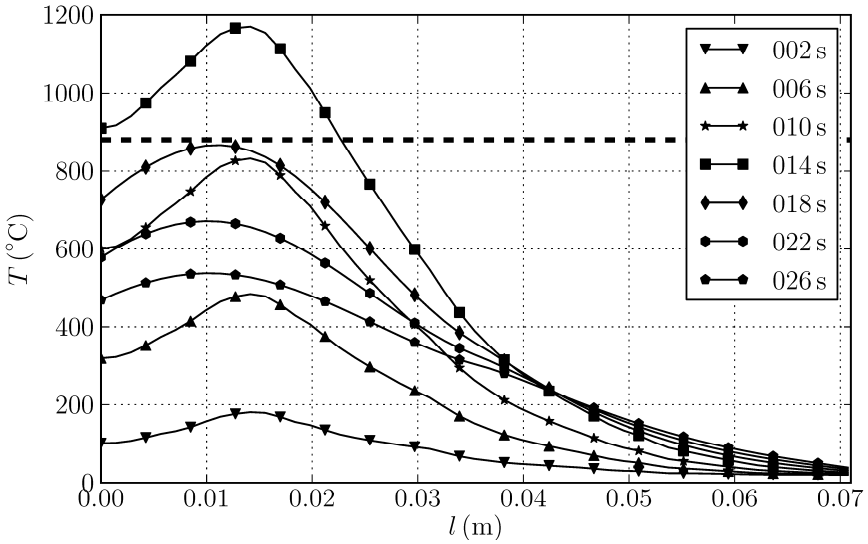

Figure 10: Distribution of the surface temperature of the hardened part (from the bottom edge) at several time levels

Figure 11 depicts the time evolution of temperature at selected point on the surface of the body. After 13 seconds we can see a sharp peak brought about by ending of the process of heating (the inductor is switched off) and immediate start of the process of intensive cooling.

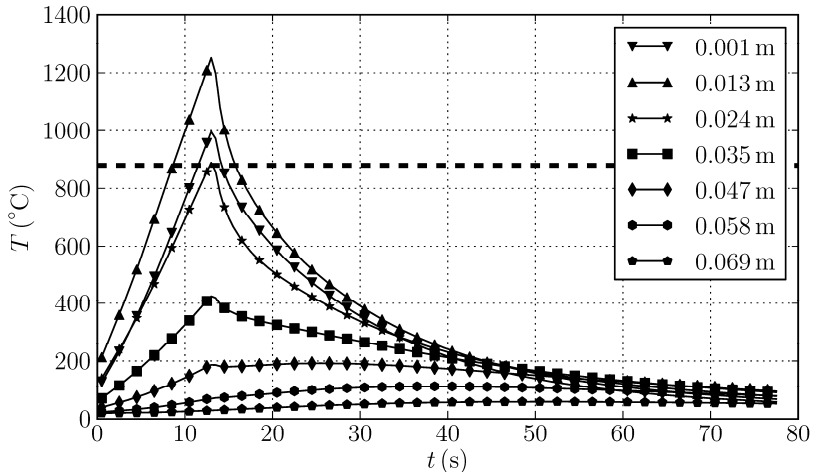

Figure 11. Time evolution of the surface temperatures at selected points of the workpiece measured from its bottom

Finally, Fig. 12 shows the distribution of temperature in the body after 10 s of heating.

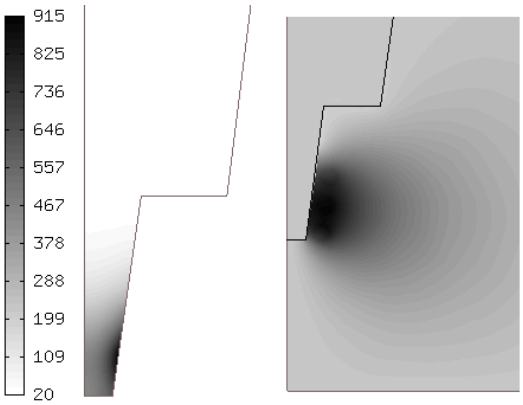

Figure 12. Distribution of the temperature in the workpiece after 10 s of heating

The time of cooling the surface from the austenite temperature Ac3 to the martensite temperature T_M is about 64 s. For this value we obtain from Fig. 7 the resultant hardness about 785 HV.

6 CONCLUSION

The numerical results are realistic and correspond to typical values obtained by experiments. The computations are relatively fast (tens of minutes), but the group plans their further acceleration using parallelization of selected parts of the code (assembly of the stiffness matrix etc.).

7 ACKNOWLEDGMENT

This work was supported by the European Regional Development Fund and Ministry of Education, Youth and Sports of the Czech Republic under the project No.

CZ.1.05/2.1.00/03.0094: Regional Innovation Centre for Electrical Engineering (RICE), by Grant project GACR P102/11/0498 and project MSMT KONTAKT MEB051041.

REFERENCES

[1] Zgraja, J. Simulation of induction hardening of flat surfaces of moving massive elements. *International Journal of Materials and Product Technology* (2007) **29**, No.1–4: 103–123.
[2] Cajner, F., Smoljan, B. and Landek, D. Computer simulation of induction hardening. *Journal of Materials Processing Technology* (2004) **157**–**158**: 55–60.
[3] Karban, P. and Donátová, M. Continual induction hardening of steel bodies. *Math. Comput. Simul.* (2010) **80**: 1771–1782.
[4] Candeo, A., Bocher, P. and Dughiero, F. Multiphysics modeling of induction hardening of ring gears for the aerospace industry. *Proc. CEFC (Electromagnetic Field Computation)* (2010), Chicago, USA, DOI 10.1109/CEFC.2010.5481552.
[5] http://hpfem.org/.
[6] Stratton, A. J. *Electromagnetic theory*. McGraw Hill, NY, 2007.
[7] Holman, *J. P. Heat transfer.* McGraw Hill, NY, 2002.
[8] Šolín, P., Segeth. K. and Doležel, I., *Higher-order finite element methods*, Chapman & Hall/CRC Press, FL, 2003.
[9] Šolín, P., Červený, J. and Doležel, I. Arbitrary-level hanging nodes and automatic adaptivity in the hp-FEM. *Math. Comput. Simul.* (2008) **77**: 117–132.
[10] Šolín, P., Červený, J., Dubcová, L. and Andrš, D. Monolithic discretization of linear thermoelasticity problems via adaptive multimesh *hp*-FEM. *J. Comput. Appl. Math.* (2010) **234**, No. 7: 2350–2357.
[11] Šolín, J., Dubcová, L. and Kruis, J. Adaptive *hp*-FEM with dynamical meshes for transient heat and moisture transfer problems. *J. Comput. Appl. Math.* (2010) **233**, No. 12: 3103–3112.